Separating the effects of heating and current drive on NTM evolution in TCV

G.M.D.Hogeweij[1*], F. Felici[2], M. Kong[2], O. Sauter[2] and the TCV team †

[1] FOM-Institute DIFFER, Association EURATOM-FOM, P.O.Box 1207, Nieuwegein, The Netherlands, www.differ.nl

[2] Ècole Fédérale Polytechnique de Lausanne (EPFL), Swiss Plasma Center (SPC), CH-1015 Lausanne, Switzerland

∗E-mail: g.m.d.hogeweij@differ.nl

Abstract.

Neoclassical Tearing Modes (NTMs) are widely observed in tokamak plasmas. They have a detrimental effect on plasma confinement and may even lead to disruptions. Therefore it is important to understand the evolution of NTMs, which is influenced by several effects. These effects are summarized in the Modified Rutherford Equation.

The TCV tokamak is equipped with very flexible heating systems and extensive magnetic and kinetic diagnostics, and is therefore very suited to study NTM evolution. In many experimental sessions at TCV the general NTM characteristics were studied.

An important question is the relative importance of the effects of heating and current drive of ECRH/ECCD on the evolution of the NTM; in many modelling efforts in the past the effect of heating was neglected. A series of dedicated TCV experiments was devoted to disentangle these roles in the suppression of the $m/n = 2/1$ NTM: the NTM was triggered by central co-ECCD using 2 gyrotrons, and then it was tried to stabilize this NTM with a third gyrotron whose deposition location was swept from the centre towards the $q = 2$ surface. In otherwise similar discharges, this third gyrotron was delivering either co- or counter-ECCD, or pure ECRH. In the experiment a clear difference in NTM stabilization was observed between these discharges.

The main aim of the present work is to reproduce the different time evolutions as described in the previous paragrah, and decide from this whether the effect of heating is essential to capture the time evolution of the NTM. This is done by simultaneously modelling the evolution of the NTMs and of the current density and temperature profiles. For this purpose the Rapid Plasma Transport simulatOR (RAPTOR) is used [F. Felici et al, *Plasma Phys. Control. Fusion* **54** (2012) 025002]. It has a module that solves the NTM evolution based on the Modified Rutherford Equation. RAPTOR self-consistently calculates the simultaneous evolution of electron temperature, q profile and NTM width.

It is shown that the triggering and suppression of the $m/n = 2/1$ NTM in TCV by varying the ECCD deposition and by varying the sign of the CD, can be described well by the Modified Rutherford Equation. Moreover, it is shown that the H term in this equation is essential to fully capture the observed dynamics.

† *See author list of S.Coda et al 2019* Nucl. Fusion ***59*** *112023*

PACS numbers: 52.25.Fi, 52.55.Fa, 52.50.Gj

1. Introduction

The need for control and stabilization of MHD instabilities in tokamak plasmas is of increasing importance, as the impact of these instabilities increases and becomes more and more detrimental for larger machines. Among these instabilities, the Neoclassical Tearing Mode (NTM) is of particular interest, as it decreases the performance of the discharge, and could eventually lead to a disruption. For values of β well below ideal MHD limits these modes are found to appear near low order resonant surfaces, giving rise to magnetic islands [1, 2]. For these reasons it is crucial to understand and control NTM evolution.

The formation of an NTM causes the temperature and density profiles to be flattened inside the islands, thus degrading plasma confinement. The pressure flattening inside the island causes a local reduction of the bootstrap current, which can sustain the mode; indeed this mechanism is the main driver of the NTM.

Localized current drive (CD) and heating (H), deposited inside a magnetic island, is a promising way to stabilize NTMs. The most useful CD and H application is ECRH/ECCD.

Theoretically, many authors have shown the effectiveness of suppressing these modes by depositing ECRH/ECCD near the flux surface where the mode is located [3, 2]. The relative merits of the heating and current drive contributions to the Modified Rutherford Equation (MRE) have also been analyzed by De Lazzari and Westerhof [4]. Recently, first principles fluid modelling of NTM stabilization by ECCD has been studied with toroidal nonlinear codes like XTOR-2F [5].

Regarding NTM control, emphasis is either on control of modes once they have grown above the detection threshold or on pre-emptive control (i.e. prevention of the development of the NTMs altogether). Many devices, e.q. ASDEX Upgrade [6], DIII-D [7], and JT-60U [8] have shown the suppression of NTMs with ECCD; in HL2-A TM and NTM stabilization by ECRH has been shown [9, 10].

Various aspects of ECRH/ECCD application for NTM control in ITER have been studied, e.g. the effect of beam width and the minimum power needed [11, 12]. The importance of good alignment of the ECRH/ECCD beam and of early detection of the mote was underlined.

TCV is equipped with a very flexible ECRH/ECCD system [13], suitable for analysis of NTM birth, growth and suppression. Moreover TCV has excellent kinetic and magnetic diagnostics, the latter being essential because magnetic perturbations are the primary fingerprint of NTMs.

In a first series of TCV experiments the general NTM characteristics were studied. It was observed that the magnetic islands are indeed of neoclassical character, i.e. they are triggered by a lack of local bootstrap current (j_{boot}). This is evidenced by the fact that they are stable if j_{boot} is too small, i.e. at low density or low input power, and that unstable NTMs are stabilized when additional local current density is provided by local heating (H) or current drive (CD). The successful modelling of the simultaneous

evolution of T_e, q and (2,1) NTM in these discharges was first reported in [14], and will be briefly summarized in this paper.

Then the main goal of this paper is to disentangle the role of heating (H) and current drive (CD) in NTM evolution. This was done by triggering the NTM with central ECRH, and then analyze the effect of heating and co- and counter-CD near the location of the NTM.

For the simultaneous modelling of the evolution of T_e, q and (2,1) NTM the Rapid Plasma Transport simulatOR (RAPTOR) [15, 16, 17] is used. it self-consistently evolves T_e, q and w_{NTM}. The effect of an NTM on plasma confinement is modelled in RAPTOR by assuming an increase of the thermal diffusion coefficient over the width of the NTM; an increase by a factor of $\simeq 2$ gives a good reproduction of the observed confinement degradation.

The experimental and modelling work in this paper fully concentrates on the (2,1) NTM; therefore, we will simply write NTM, always referring to the (2,1) NTM.

This paper is organized as follows. Section 2 describes the experimental set-up and observations. Then section 3 deals with various aspects of NTM evolution: experimental estimation of NTM width, the Modified Rutherford Equation (MRE), and the comparison of the relative importance for the NTM evolution of the Current Drive (CD) and Heating (H) terms in the MRE. Section 4 treats in detail the way transport and NTM evolution have been modelled, which is followed by the modelling results in section 5. Finally, in section 6 the results are discussed, some conclusions are drawn and an outlook is sketched.

2. Experimental set-up and observations

The general set-up of the experiments was based on low- to medium density, high q_a ohmic target plasmas in TCV ($\langle n_e \rangle \sim 1 - 2 \cdot 10^{19} \mathrm{m}^{-3}$, $q_a \sim 10$). After the ohmic target plasma had been established central ECRH/ECCD was applied with 1 or usually 2 gyrotrons, in order to trigger the NTM. Then a third gyrotron was used in swept mode, to study suppression of the NTM.

In a first series of experiments the general characteristics of NTMs in TCV were studied. It was found that the centrally localized heating provided by 1-2 gyrotrons (each delivering typically 0.4-0.5 MW) was sufficient to trigger the NTM, unless the density was too low. Moreover, it was shown that the heating and current drive of 1 gyrotron with power deposition close to the $q = 2$ surface, very reliably stabilizes the NTM. some examples are shown in Fig.1.

In 2016 dedicated experiments were performed in TCV to study NTM evolution and suppression, and to disentangle the roles of heating (H) and current drive (CD) in the stabilization. In these experiments 2 gyrotrons with co-ECCD with nearly central deposition were applied to trigger the NTM, and then a third gyrotron was switched on with swept power deposition location, delivering co- or ctr-ECCD or pure ECRH. Experimental observations are summarized in figures 2,3.

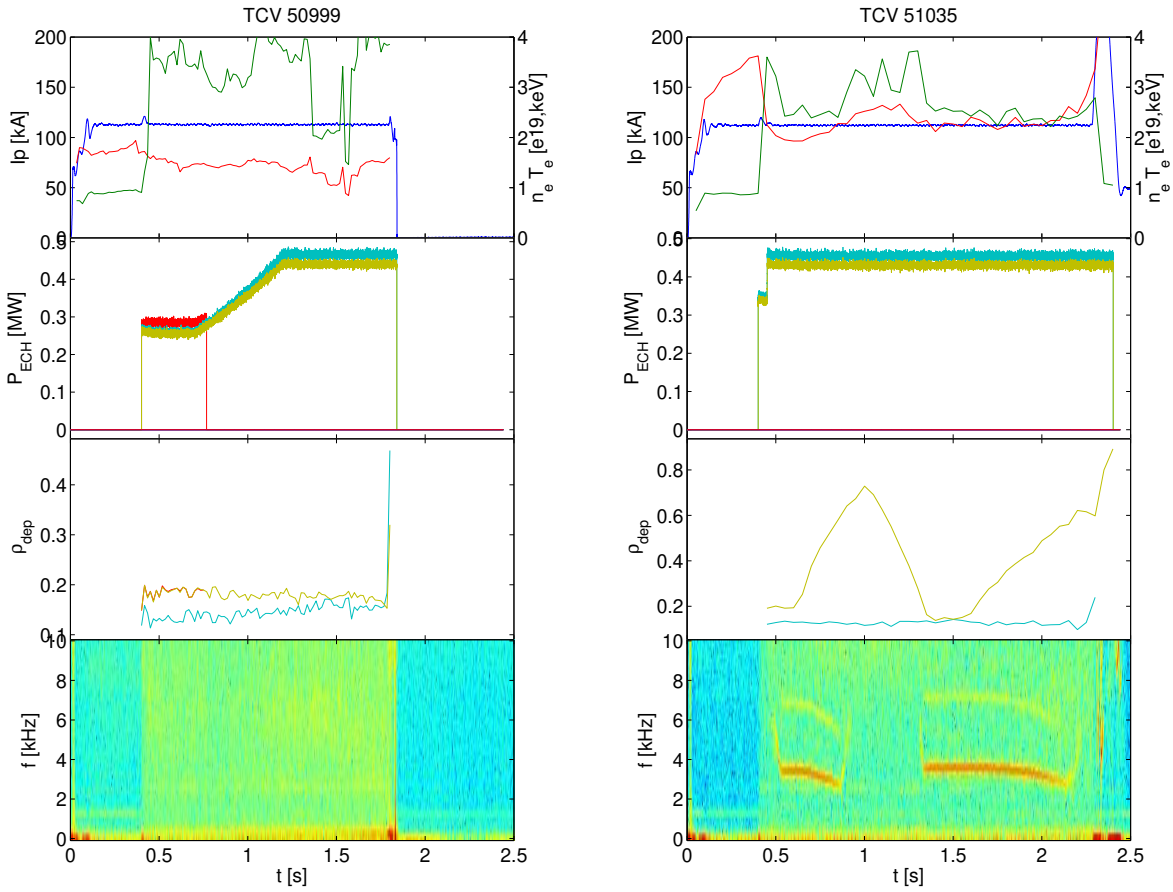

Figure 1. *Time traces of I_p (blue), central n_e (red) and T_e (red) (upper panel), P_{ECH} and ρ_{dep} of the 2 or 3 gyrotrons used (middle and lower panels), and the MHD spectrogram for discharges #50999 and #51035. One of the gyrotrons (the one with the pale green time traces) delivered co-ECCD. In the low-density case #50999 no NTM was triggered. The medium density case #51035 showed both triggering of a 2/1 NTM by the EC heating, and suppression when the ECCD was close to the location of the NTM.*

3. NTM evolution

3.1. Estimation of NTM width

The RAPTOR modelling presented in section 5 not only yields the evolution of the T_e and q profiles, but also the evolution of the NTM width. Hence, in order to verify these modelling results it is important to have an experimental estimate of the NTM width. One way to assess the NTM width is from the drop of β_N due to the NTM:

$$\omega_{sat} = \frac{\Delta\beta_N}{\beta_N}\frac{1}{4{\rho_{mn}}^3} \tag{1}$$

where ρ_{mn} and ω_{sat} are the radii of the resonant surface and the saturated island width, respectively, both normalized to minor radius [18]. From an estimated $\Delta\beta_N \sim 8-10\%$ and a typical location of the (2,1) NTM at $\rho_{mn} = 0.4 \sim 0.5$ we find typically $w_{sat} \simeq 5\pm1$ cm for the fully developed NTM.

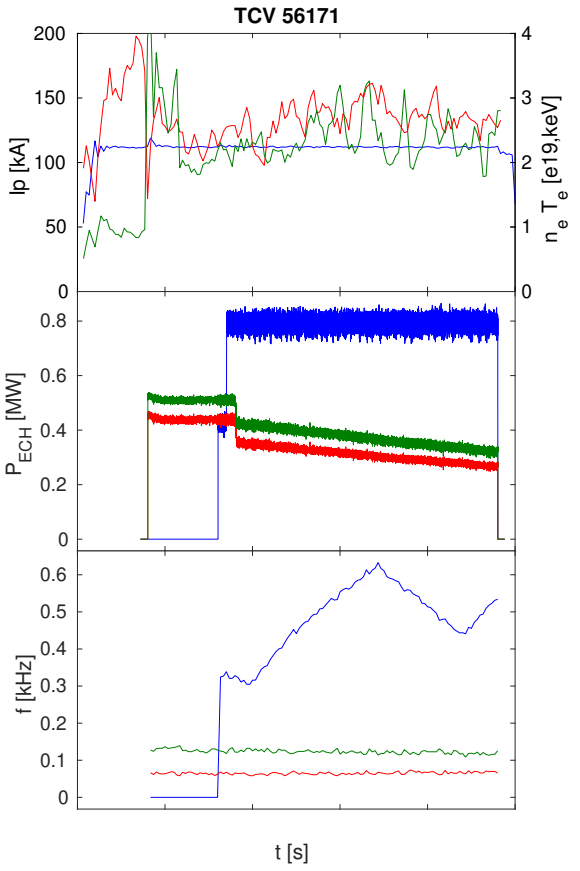

Figure 2. *Time traces of I_p, central n_e and T_e (upper panel), P_{ECH} and ρ_{dep} of the 3 gyrotrons (middle and lower panels), for TCV shot #56171 (the other two shots have identical time traces).*

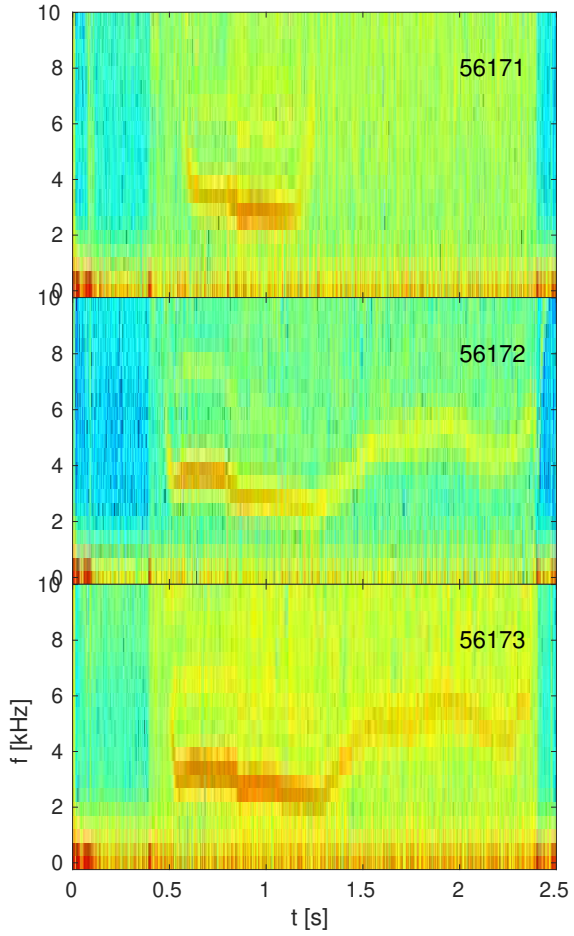

Figure 3. *MHD spectrograms for shots #56171 (co CD), #56172 (ctr CD), and #56173 (pure heating), showing full NTM suppression in the first shot and partial suppression in the other two shots.*

Moreover, the relative NTM width is directly related to the magnetic mode amplitude: $w_{NTM} \simeq \tilde{B}^{0.5}$. The mode amplitude can be derived from the Power Spectral Densities (PSDs) of magnetic pick-up coil signals; Fig.4 shows these for the three discharges 56171, 56172 and 56173. The PSD of discharge 56171 shows full suppression of the mode after $\simeq$ 1.2 s; apparently the noise level of the signal corresponds to a mode amplitude of $\sim 2 \cdot 10^{-3}$. The PSDs show a clear reduction of the NTM width for discharges 56172 and 56173 when ρ_{dep} comes close to the NTM, but no full suppression is attained in these cases. The trends shown in the mode amplitudes are in good agreement with the MHD spectra of Fig.3. It should be noted that the PSDs only give the relative width of the NTM, so these signals are useful to assess the trend, e.g. whether there is partial suppression. For an absolute width, one needs the β_N drop, as described in the previous paragraph.

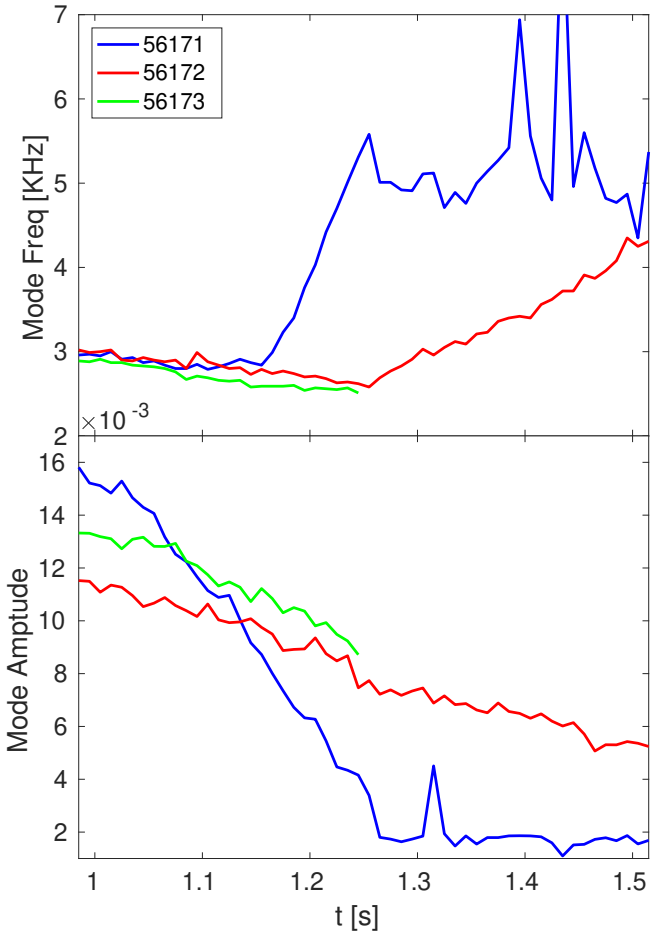

Figure 4. *Time traces of mode frequency and amplitude for the shots #51671/2/3, as determined from Power Spectral Densities, showing full suppression in the first case and reduction of the NTM by ∼ 30% in the other 2 cases. Due to a numerical problem the run for shot #51673 was not completed.*

3.2. Modified Rutherford Equation

Theoretically the time evolution of an NTM is described by the Modified Rutherford Equation (MRE) [18]. The MRE can be cast in various forms; we follow here the conventions of [4, 19]. In their description there are 5 terms in evolution of NTM width, viz. the classical, bootstrap, Glasser-Green-Johnson (GGJ), current drive (CD), and heating (H) term:

$$\frac{dw}{dt} = \frac{{r_{\rm mn}}^2}{\tau_{\rm R}}(\Delta'_{\rm class}(w) + \alpha_{\rm BS}\Delta'_{\rm BS}(w) + \alpha_{\rm GGJ}\Delta'_{\rm GGJ}(w) + \alpha_{\rm CD}\Delta'_{\rm CD}(w) + \alpha_{\rm H}\Delta'_{\rm H}(w)) \quad (2)$$

where $r_{\rm mn}$ is the radius of the resonant surface and $\tau_{\rm R}$ is the resistive time [19], and where the five driving terms $\Delta'_{\rm class,BS,GGJ,CD,H}$ are all given by prescribed formulas. In principle all $\alpha_{\rm BS,GGJ,CD,H} = 1$. However uncertainties in experimental data and possible approximations in derivations call for introduction of these terms ~ 1.

3.3. Classical or Neoclassical Tearing Mode?

The classical term or tearing parameter is given by the jump in the logarithmic derivative of the radial magnetic field at the rational magnetic surface, and is mainly driven by

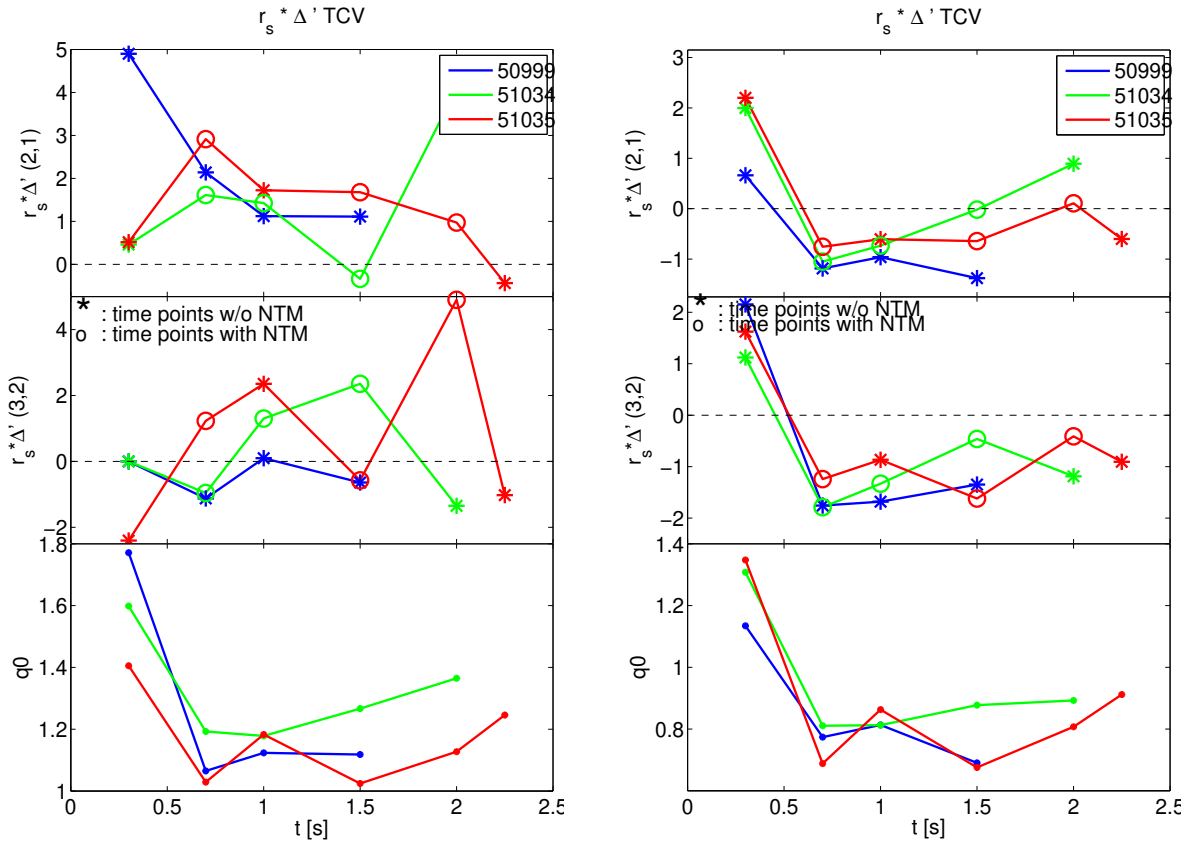

Figure 5. *Calculated values of* $r_{\rm mn}\Delta'_{\rm class(0)}$ *for selected time points of 3 TCV discharges: 5099, 51034 and 51035. The calculations used q profiles from equilibrium reconstruction (left panel), and from RAPTOR simulations; in the latter case RAPTOR was run with suppression of the NTMs, in order to have the value of* $r_{\rm mn}\Delta'_{\rm class}$ *for a plasma without NTM. The results of both calculations are contradictory.*

the equilibrium current gradient [1]. It can be written as:

$$r_{\rm mn}\Delta'_{\rm class}(w) = r_{\rm mn}\Delta'_{\rm class}(0) - (m + r_{\rm mn}\Delta'_{\rm class}(0)f(w) \tag{3}$$

with

$$f(0) = 0, \frac{df}{dw}(0) = \alpha_{\rm CL}, \lim_{w\to\infty} f(w) = 1 \tag{4}$$

An important question is the sign of the tearing parameter $\Delta'_{\rm class}$ before the onset of the mode, i.e. at $w = 0$. If $\Delta'_{\rm class}(0) > 0$ the current profile itself drives the mode unstable; if $\Delta'_{\rm class}(0) < 0$ another term must drive the mode, and this can only be the bootstrap term (the GGJ term is always stabilizing), i.e. the mode is of neoclassical character (and is called an NTM).

It is possible to calculate $\Delta'_{\rm class}(0)$ from the q profile. Unfortunately, $\Delta'_{\rm class}(0)$ is critically dependent on dq/dr, and the q profile is not known accurately. In TCV there are no direct measurements of the q profile, so one has to rely on the equilibrium reconstruction, which is not able to capture peculiarities like hollow current density

profiles. Using this, one finds at most time points $\Delta'_{\rm class}(0) > 0$. Alternatively, one can use the q profile from RAPTOR simulations; at most time points this yields $\Delta'_{\rm class}(0) < 0$, see Fig.5. So calculations are inconclusive in this matter.

Therefore it is more useful to consider experimental evidence. As an NTM is observed neither in the ohmic phase nor in low density EC heated cases, $\Delta'_{\rm class}(0)$ cannot be $\gg 0$. A tiny NTM, of which the magnetic fingerprint is hidden in the noise, may well exist in these phases, so a value of $\Delta'_{\rm class}(0)$ just above 0 cannot be excluded. On the other hand, these TCV discharges are in L-mode and with low $I_{\rm p}$. Hence there are no or tiny sawteeth and no ELMs, so there are no seed islands; hence a mode could never be triggered if $\Delta'_{\rm class}(0) \ll 0$. Again, there might be some low level magnetic turbulence which could give rise to tiny seed islands, just enough to trigger a mode even when $\Delta'_{\rm class}(0)$ is just below 0. However, there is no sign of such turbulence, therefore we conclude that $\Delta'_{\rm class}(0)$ is close to 0, and probably small positive; this was also stated in [20]). It means that the real driving term is the bootstrap term, i.e. that indeed the modes are of neoclassical character, so the term NTM is justified.

3.4. Comparison of CD and H terms in NTM evolution:

The CD and H terms in the MRE have the same structure:

$$\Delta'_{\rm CD,H} \simeq \eta_{\rm CD,H}(w_{\rm dep}, \chi_{\rm e}^{\rm ins}) N_{\rm CD,H}(w) G_{\rm CD,H}(w, x_{\rm norm}) M_{\rm CD,H}(w, D) \tag{5}$$

where $w_{\rm dep}$ is the deposition width, $\chi_{\rm e}^{\rm ins}$ is $\chi_{\rm e}$ inside the island, $w \equiv w_{\rm NTM}/w_{\rm dep}$ is the normalized island width, and

$$x_{\rm norm} \equiv |(r_{\rm dep} - r_{\rm mn})|/max(w_{\rm dep}, w_{\rm NTM}) \tag{6}$$

is the normalized misalignment of the power deposition with respect to the island, and η, N, G, M and D are the efficiency, normalization factor, geometry factor, modulation effect, and duty cycle, respectively. The latter is not considered here - only CW ECH/ECCD is applied, i.e. duty cycle $D = 1$, hence $M = 1$.

The reader is referred to [4, 19] for the various formulas. We only want to recall here $G_{\rm CD}$, where following analytical form was proposed in [19] to emulate the numerical results of [4]:

$$G_{\rm CD} = (1 + G_{\rm coeff}) \frac{1 - \tanh(3.75 x_{\rm norm} - 1.5)}{1 - \tanh(-1.5) + 2 {x_{\rm norm}}^3} - G_{\rm coeff} e^{-{x_{\rm norm}}^2} \tag{7}$$

where $G_{\rm coeff} = 0.6$. Fig.6 shows $N_{\rm CD,H}$ as function of $w/w_{\rm dep}$ and $G_{\rm CD,H}$ as function of $x_{\rm norm}$. The destabilizing action of misaligned CD (when $x_{\rm norm} \geq 0.5$) is provided by the second term of Eq.7. Putting $G_{\rm coeff} = 0$ cancels this destabilizing effect, as shown by the cyan curve in the lower panel of Fig.6.

To get a flavour of the relative contributions of the 5 terms to the MRE, we have done two simulations with fixed $w_{\rm NTM}$, see Fig.7. It is assumed that inside the island

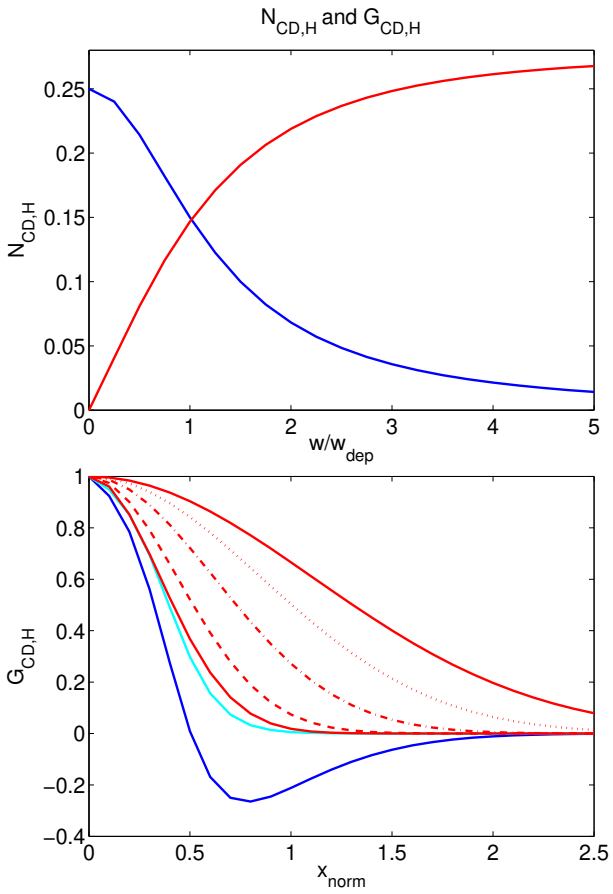

Figure 6. *Normalization and geometry factor for CD (blue) and H terms (red), as function of w and $x_{\rm norm}$. In the lower plot various widths of the NTM are assumed, from 0 (narrowest curve) to 5 cm (widest curve). Note that $G_{\rm H}$ is always positive whereas $G_{\rm CD} < 0$ (i.e. destabilizing) for misaligned power. Cyan curve in lower panel: adapted $G_{\rm CD}$ such that destabilizing effect is cancelled (see text).*

$\chi_{\rm e}$ is strongly reduced, as has been observed [21]. In the runs a reduction by a factor of 50 is assumed, which is about the ratio between anomalous and neoclassical value if $\chi_{\rm e}$.

It is seen that under favourable conditions (large island, low $\chi_{\rm e}^{\rm ins}$) $\Delta'_{\rm H} \simeq \Delta'_{\rm CD}$. Moreover, Fig.7 shows that for large $w_{\rm NTM}$ the destabilizing CD term for strongly misaligned ECCD, is compensated by the stabilizing H term. It should be noted that this, of course, is only true for co-CD; for counter-CD the CD term is stabilizing for strongly misaligned ECCD.

In literature, e.g. [19], the H term in the MRE is often neglected. One reason may be that this term does not play a role in the triggering of the NTM, and only becomes large for a well-developed island with low thermal diffusion inside. A second reason is that the H term critically depends on $\chi_{\rm e}^{\rm ins}$, which is normally not known.

In this paper, therefore, we will simulate NTM evolution in 3 ways. First, by simply omitting the H term. Second, by emulating the effect of the H term by using an adapted $G_{\rm CD}$ without destabilizing effect of misaligned CD (cyan curve in Fig.6); as noted before, this only makes sense for co-CD. And third, by using the full MRE including the H term, and assuming a strongly reduced thermal diffusion inside the island.

It is worthwhile noting that Fig.7 also shows that, for well-aligned ECH/ECCD, the H and CD terms are much stronger than any other term. So indeed, once the power deposition is close the the NTM location, ECH/ECCD is by far the dominant player in

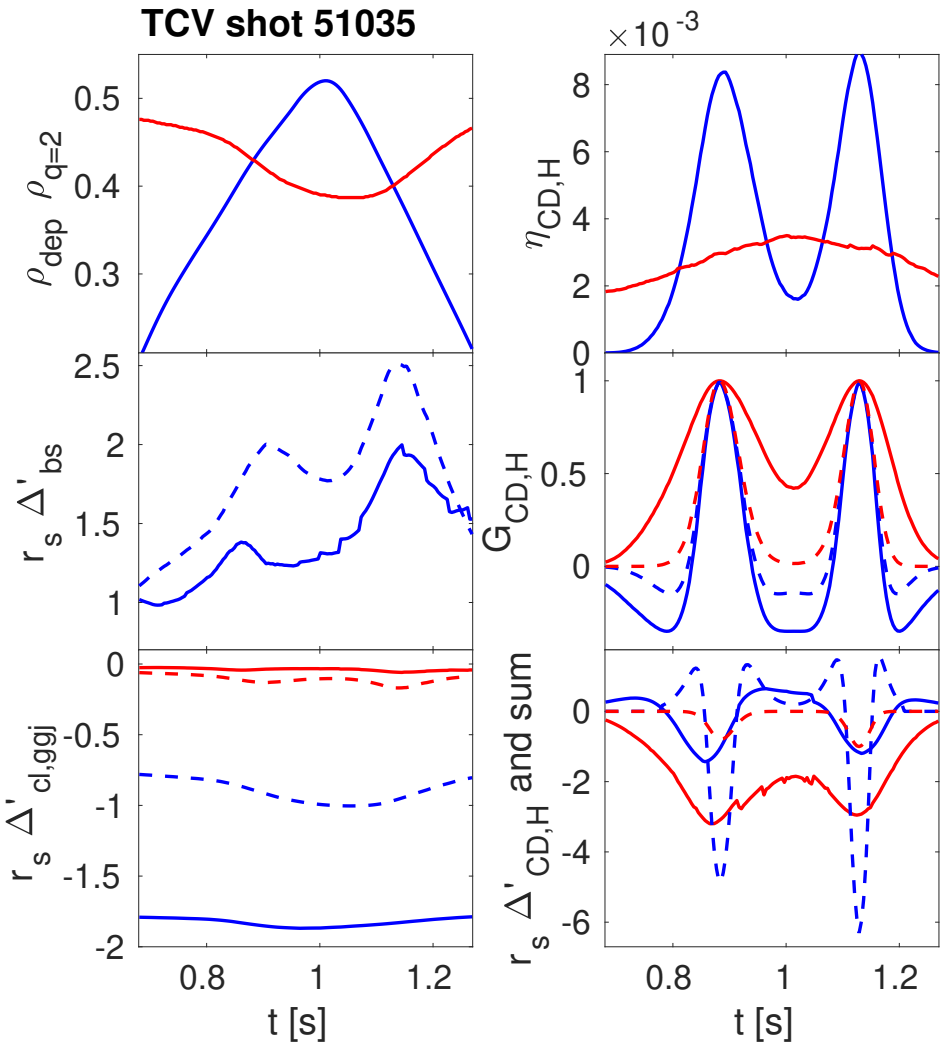

Figure 7. *Various terms of the MRE for a discharge with a strong sweep of* $\rho_{\rm dep}$ *(shown in upper left panel), assuming fixed* $w_{\rm NTM} = 1.5$ *(dashed) and 5 cm (full curves). In the lower left frame the classical term is plotted in blue, the GGJ term in red. In all right-hand frames the CD terms are in blue, the H terms in red. For the calculation of* $\eta_{\rm H}$ *it is assumed that* $\chi_{\rm e}^{\rm ins}$ *is a factor of 50 lower than outside the island.*

the NTM evolution.

4. Transport and MHD modelling

RAPTOR self-consistently calculates the simultaneous evolution of $T_{\rm e}$ and q profiles and NTM width. For the power balance all sources are taken into account, in these discharges ECRH and ohmic heating, where the latter is calculated self-consistently. For each gyrotron the power deposition location is calculated by ray tracing for each time point; the power deposition profiles are assumed to be of Gaussian shape with full width half width 0.15 or 0.2 of the minor radius, in agreement with calculations.

RAPTOR takes $n_{\rm e}$ from experiment. There are no $T_{\rm i}$ measurements available, for

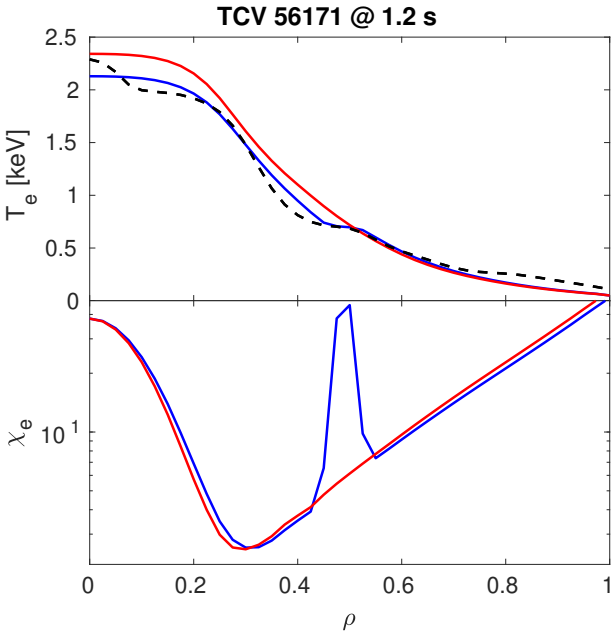

Figure 8. *T_e and χ_e profiles at 1.2 s for TCV shot 56171, for RAPTOR runs without NTM (red) and with NTM-enhanced χ_e with A_{mn}/C_{mn} = 8.0/0.5 (m=2,n=1,blue). The experimental T_e profile is also shown (black dashed curve).*

these TCV discharges, hence for T_i an educated guess is taken; note, however, that in typical TCV plasmas the electron-ion coupling is weak due to the low density and small size of the machine, so any error in the assumed T_i will only marginally affect the electron power balance. Prescribed (CHEASE) equilibria are used (calculated for various time slices). RAPTOR has a module that solves the NTM evolution based on the MRE. In RAPTOR χ_e is prescribed semi-empirically, with several parameters tunable for different plasma regimes.

The effect of an (m, n) NTM on plasma confinement in RAPTOR is modelled by assuming an increase of χ_e over an area proportional to the NTM width [22]:

$$\chi_e^{mn}(\rho) = \chi_e(\rho)(1 + A_{mn} exp(\frac{-4(\rho - \rho_{mn})^2}{C_{mn}(w_{NTM}/a)^2} \tag{8}$$

A_{mn} and C_{mn} are assessed by using in RAPTOR a prescribed NTM width as estimated in experiment, and fine-tuned such that the simulated reduction of both T_e and β_N matches experimental observations. The best simulated reduction of T_e and β_N was obtained by taking a strong χ_e enhancement over a relatively narrow region, see Fig.8.

5. Results

We first concentrate on discharge 56171, i.e. the one with co-CD. Figure 9 shows the NTM width evolution for the 3 assumptions discussed before: *(i)* without H-term and standard CD-term; *(ii)* without H-term and adapted CD-term; *(iii)* with H-term included and standard CD-term. It is clearly seen that in the first case the simulation is incorrect, as it predicts an NTM during the period that ρ_{dep} is much larger than $\rho(q = 2)$. This can be understood as a consequence of the destabilizing action of the CD

as soon as $x_{\rm norm}$ exceeds $\simeq 0.5$. This effect, not observed in the experiment, is avoided in the simulations either by the artificial cancellation of this destabilizing action of the misaligned CD, or by counteracting it by the H term; indeed, both methods lead to nearly identical results.

It should be noted that the three simulations shown in Fig.9 used otherwise identical parameters. In particular, in the MRE was used:

$$r_{\rm mn}\Delta'_{\rm class}(0) = 0.3; \alpha_{\rm BS} = 2.1; \alpha_{\rm GGJ} = 0.5; \alpha_{\rm CD} = 1 \qquad (9)$$

The result shown here is typical for all discharges where the deposition location of one gyrotron is swept until a value far outside $\rho(q = 2)$; e.g. simulations for discharge 51035 (see Fig.1) showed the same picture.

From this exercise one can conclude that just omitting the H term in the MRE does not fit the experimental results. Therefore we now concentrate on simulations where the effect of the H term is emulated by a modified CD term. Under these assumptions, using the same numerical values as before, results for the 3 discharges considered were

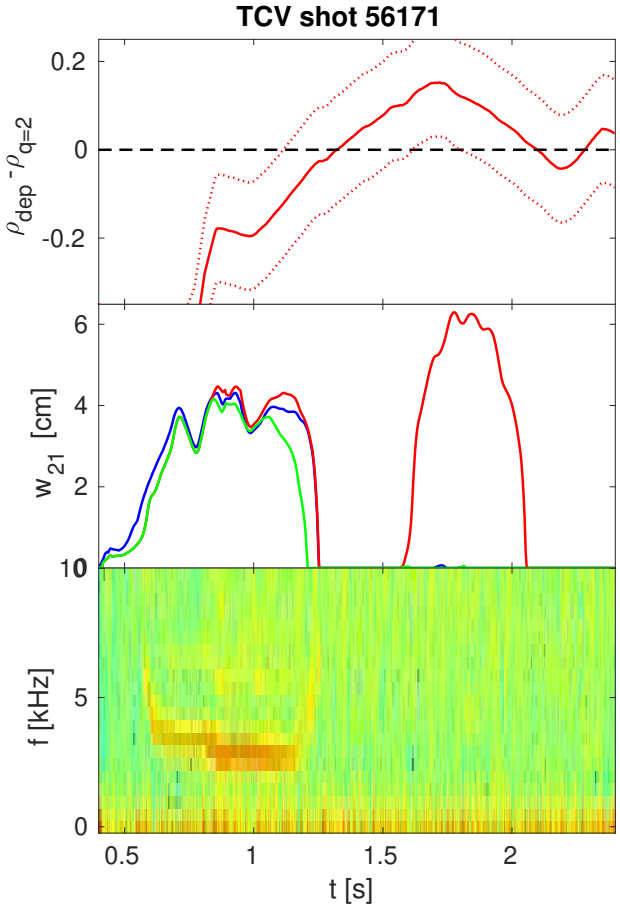

Figure 9. *RAPTOR simulations for #56171 in middle panel: Blue: no H-term, with adapted $G_{\rm CD}$ Red: no H-term, with standard $G_{\rm CD}$ Green: with H-term, with standard $G_{\rm CD}$ Upper panel shows $\rho_{\rm dep} - \rho(q = 2)$ (full line), and this value $\pm w_{\rm dep}$ (dashed lines).*

The simulated size of the NTM is realistic, although a bit high for pulses 56172 and 56173 (remind that from the loss of $\beta_{\rm N}$ a width of 5 ± 1 cm was estimated). The full suppression of the NTM in pulse 57171 is correctly predicted, and at the right time. In

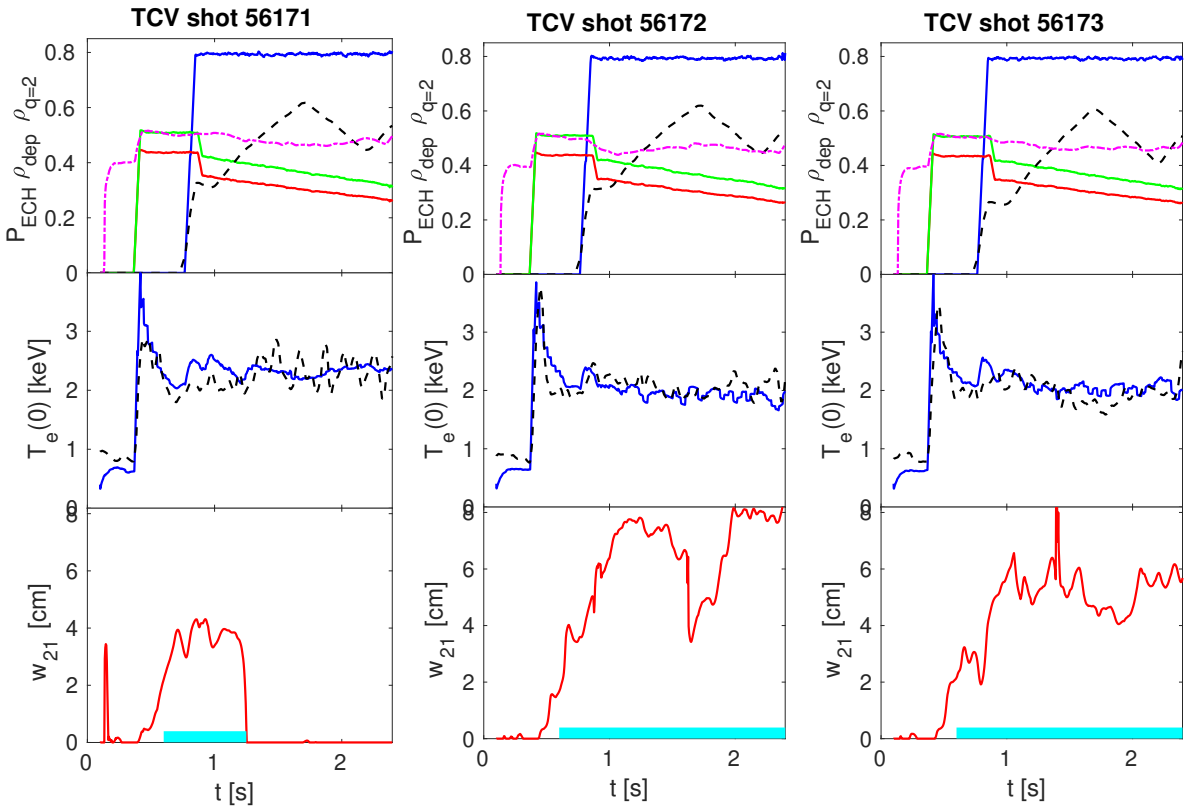

Figure 10. *RAPTOR simulations for #56171,-72,-73, no H-term, with adapted* G_{CD}*. Upper: Powers of central (red, green) and off-axis gyrotron (blue),* ρ_{dep} *of the latter (dashed) and* $\rho(q=2)$ *(magenta). Middle:* $T_{\mathrm{e}}(0)$ *from experiment (dashed) and simulation (full blue); in the 1st plot* $T_{\mathrm{e}}(0)$ *is also shown for a run without NTM (red). Lower:* w_{NTM} *from the simulations (red); the cyan bar indicates when the NTM was present in the experiment.*

the simulation of pulses 56172 and 56173 the NTM is not suppressed, in agreement with experiment; however, the reduction of NTM size (i.e. partial suppression) in these pulses, observed when the ECH deposition is close to the NTM location, is not reproduced by the simulations.

Now turning to the ctr-ECCD case, pulse 56172, Fig.11 shows that including the H-term in the simulation has two effects: first, the size of the NTM during its full development is reduced to ~ 5 cm, in agreement with experiment; second, the observed partial suppression when ρ_{dep} is close to $\rho(q=2)$, is now correctly reproduced by the simulation. So only the inclusion of the H-term allows realistic simulation of this discharge.

Finally, turning to the pure heating case, pulse 56173, Fig.12 shows that inclusion of a weak H-term (i.e. with a relatively high value of $\chi_{\mathrm{e}}^{\mathrm{ins}}$) already leads to a reduction of the NTM to a more realistic size (red curve). If a strong reduction of $\chi_{\mathrm{e}}^{\mathrm{ins}}$ is assumed (by a factor of 50 relative to the anomalous χ_{e} outside the island), then again partial suppression of the NTM is observed when ρ_{dep} is close to $\rho(q=2)$, in agreement with

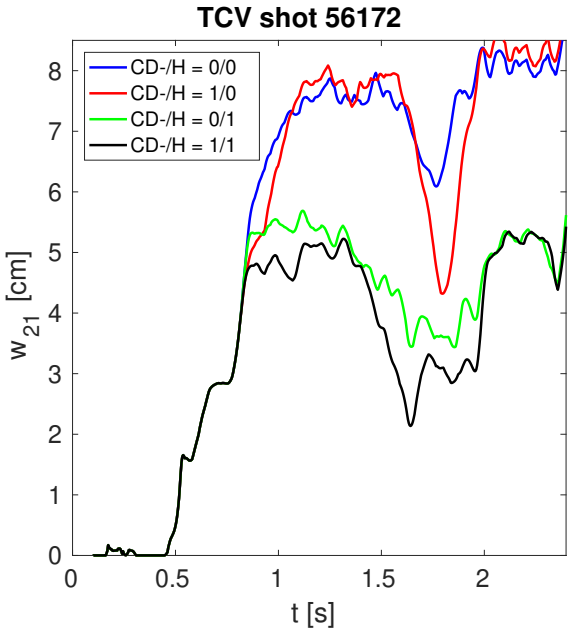

Figure 11. *w_{NTM} for RAPTOR simulations for #56172 with all combinations of with/without H-term with/without adapted G_{CD}, showing that with the H-term w_{NTM} is reduced to more realistic values, and also is further reduced when the power deposition is close to the NTM, in agreement with experimental observation (see Fig.3).*

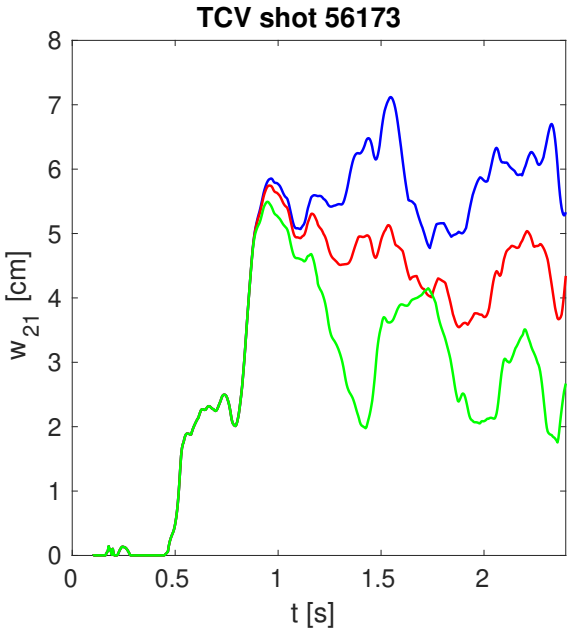

Figure 12. *w_{NTM} for RAPTOR simulations for the pure heating case #56173, with no H-term (blue) and with various strengths of the H-term (red, green). The latter simulation (green) shows partial suppression of the NTM when ρ_{dep} is close to the NTM, in agreement with experimental observation (see Fig.3).*

experimental findings.

So concluding these simulation results, it has been shown that for co-ECCD discharges like #56171, the simplified modelling without H-term and adapted G_{CD} yields results as good as the full modelling including the H-term. However, for the ctr-ECCD case #56172 and pure ECH-case #56173, only the full modelling both yields a realistic width of the NTM, and reproduces the partial suppression of the NTM when ρ_{dep} is close to $\rho(q = 2)$.

The strength of the results shown here is that they are the outcome of selfconsistent simulations of the simultaneous evolution of T_{e}, q and NTM. As shown in Fig.13, indeed the T_{e} profiles from the RAPTOR simulations capture well the experimental T_{e} profiles, including the local flattening due to the presence of an NTM. There are no direct measurements of the q profile in TCV; however, the fact that, when an NTM is present, the flat spot in the T_{e} profile in the RAPTOR simulation is at the same radial position as in the experimental data, proves that at least the location of the $q = 2$ surface is correct in the simulations.

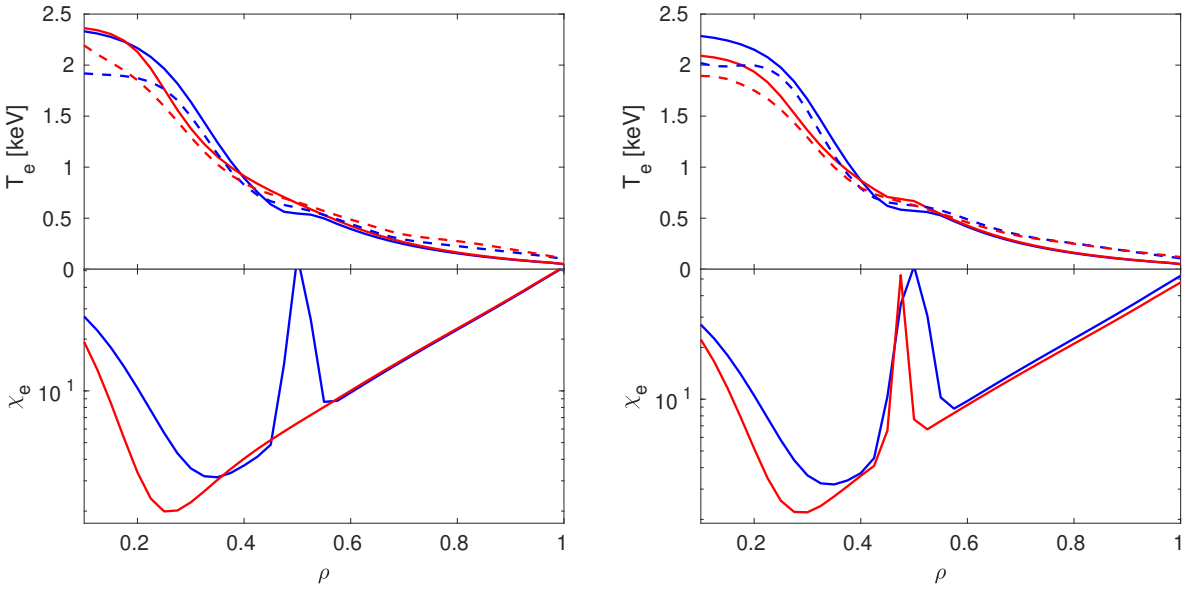

Figure 13. *Profiles of T_e (upper frames) and χ_e (lower frames) at specific time points for discharges 56171 (left) and 56173 (right). Profiles are shown at time of full NTM development at 0.9 s (blue), and at time of full and partial NTM suppression (56171 and 56173, respectively) at 1.4 s (red). Measured T_e profiles are dashed lines; results of RAPTOR simulations are full lines. To get rid of noise in the experimental data, the measured T_e profiles shown have been averaged over a time window of 0.1 s around the given time point. The flattening of T_e due to the NTM is seen on both the measured and simulated profiles; the identical location of both indicates that the location of the $q = 2$ surface in the RAPTOR simulations is correctly calculated.*

6. Discussion and Conclusions

In this work it has been shown that the simultaneous evolution of T_e and q profile and (2,1) NTM width can be selfconsistently simulated in TCV discharges with both co- and counter-ECCD and pure ECH. Three versions of the MRE were compared: (a) a version without taking into account the effect of EC heating on the NTM evolution (the so-called H-term in the MRE); (b) a version still without H-term but with adapted CD-term; (c) the full version. It has been shown that version (a) does not correctly reproduce discharges with co-ECCD, and that both other versions do reproduce such discharges very well. For the ctr-ECCD and pure-heating case, only the full version of the MRE captures the NTM width in detail.

It should be noted that in the most recent version of RAPTOR also the T_i evolution can be simulated, using a simple semi-empirical prescription for χ_i [17]. This version was not used in the simulations shown in this paper, because no T_i measurements were available for the discharges considered. However, due to the low density and pure electron heating, $T_i \ll T_e$ and the electron-ion coupling is weak, so any error in the estimated T_i would have a marginal effect on the electron power balance.

NTM stabilization experiments and modelling is an active research area on many

tokamaks. E.g. on AUG similar experiments in AUG have been done [23]. Similar modelling is being done for ITER, using coupled TRANSP and TORBEAM for the kinetic and NTM evolution, respectively [12], however, without taking into account the H-term.

Some notes are in place regarding NTM control in ITER. Of course, in an ideal world NTMs would be completely preempted, which could be achieved by continuous application of perfectly aligned ECRH/ECCD. For this purpose ECCD is ideally suited, with a strong stabilizing effect of the CD term provided perfect alignment; the effect of heating does not play a role here (the H-term vanishes for $w_{\mathrm{NTM}} = 0$). However, permanent ECCD may not be available (it may be needed for other purposes), and perfect alignment will often not be achieved. So it is likely that NTMs do show up, and may grow rapidly before they have been detected and the ECCD launchers have been steered to the right position. In this phase the heating effect will be very helpful, since it already starts to stabilize the NTM as soon as some of the power enters the island, i.e. well before the ECCD/ECRH system has been steered to perfect alignment. So the heating effect may be very beneficial in preventing the NTM from unacceptable growth, and it is important to take it into account when modelling application of ECRH/ECCD for NTM stabilization in ITER.

Finally, it should be noted that understanding and prediction of NTM evolution is essential in setting up reliable control schemes. In TCV NTM control has been integrated with multiple controllers in TCV [24] and is being used for disruption avoidance [25], finally leading to complete real-time plasma state monitoring [26].

References

[1] O. Sauter *et al*, *Phys. Plasmas* **4** (1997) 1654
[2] R.J. La Haye *et al*, *Phys. Plasmas* **13** (2006) 055501
[3] C.C. Hegna *et al*, *Phys. Plasmas* **4** (1997) 2940
[4] D. De Lazzari *et al*, *Nucl. Fusion* **49** (2009) 075002
[5] O. Fevrier *et al*, *Plasma Phys. Control. Fusion* **58** (2016) 045015
[6] G. Gantenbein *et al*, *Phys. Rev. Lett.* **85** (2000) 1242
[7] R. Prater *et al*, *Nucl. Fusion* **47** (2007) 371
[8] A. Isayama *et al*, *Nucl. Fusion* **41** (2001) 761
[9] J. Cheng *et al*, *Phys. Lett A* **380** (2016) 3897
[10] Jingchun Li *et al*, *Phys. Plasmas* **26** (2019) 032505
[11] Minho Park *et al*, *Nucl. Fusion* **58** (2018) 016042
[12] F.M. Poli *et al*, *Nucl. Fusion* **58** (2018) 016007
[13] T.P. Goodman *et al*, *Nucl. Fusion* **48** (2008) 054011
[14] G.M.D. Hogeweij *et al*, poster at EU-US TTF meeting, Leysin, Switzerland, September 2016
[15] F. Felici *et al*, *Plasma Phys. Control. Fusion* **54** (2012) 025002
[16] P. Geelen *et al*, *Plasma Phys. Control. Fusion* **57** (2015) 125008
[17] F. Felici *et al*, *Nucl. Fusion* **58** (2018) 096006
[18] O. Sauter *et al*, *Plasma Phys. Control. Fusion* **52** (2010) 025002
[19] O. Sauter *et al*, *Details on the expressions used in the various terms of the modified Rutherford equation (2015)*, included in the RAPTOR documentation, https://crppsvn.epfl.ch/wsvn/RAPTOR/tags/release-1.3/

[20] H. Reimerdes *et al*, *Phys. Rev. Lett.* **88** (2002) 105005
[21] G.W. Spakman *et al*, *Nucl. Fusion* **48** (2008) 115005
[22] G. Turri *et al*, Proc. 22nd FEC, Geneva, 2008, EX/P3-6
[23] H. van den Brand *et al*, *Nucl. Fusion* **59** (2019) 016003
[24] M. Kong *et al*, Proc. 44th EPS Conference, Belfast, UK, 2017 P4.152
[25] U.A. Sheikh *et al*, *Nucl. Fusion* **58** (2018) 106026
[26] T.C. Blanken *et al*, *Nucl. Fusion* **59** (2019) 026017

Acknowledgements

This work, supported by the European Communities under the contract of Association between EURATOM/F0M, was carried out within the framework of the European Fusion Programme with financial support from NWO. The views and opinions expressed herein do not necessarily reflect those of the European Commission. This work was supported in part by NWO-RFBR Centre-of-Excellence on Fusion Physics and Technology (Grant nr. 047.018.002) and by the Swiss National Science Foundation.